Research Article Open Access

G. Ariu*, I. Hamerton, and D. Ivanov

Positioning and aligning CNTs by external magnetic field to assist localised epoxy cure

DOI 10.1515/phys-2016-0057
Received August 15, 2016; accepted November 23, 2016

Abstract: This work focuses on the generation of conductive networks through the localised alignment of nano fillers, such as multi-walled carbon nanotubes (MWCNTs). The feasibility of alignment and positioning of functionalised MWCNTs by external DC magnetic fields was investigated. The aim of this manipulation is to enhance resin curing through AC induction heating due to hysteresis losses from the nanotubes. Experimental analyses focused on in-depth assessment of the nanotube functionalisation, processing and characterisation of magnetic, rheological and cure kinetics properties of the MWCNT solution. The study has shown that an external magnetic field has great potential for positioning and alignment of CNTs. The study demonstrated potential for creating well-ordered architectures with an unprecedented level of control of network geometry. Magnetic characterisation indicated cobalt-plated nanotubes to be the most suitable candidate for magnetic alignment due to their high magnetic sensitivity. Epoxy/metal-plated CNT nanocomposite systems were validated by thermal analysis as induction heating mediums. The curing process could therefore be optimised by the use of dielectric resins. This study offers a first step towards the proof of concept of this technique as a novel repair technology.

Keywords: Multi-walled carbon nanotubes, high conductivity connections, electroless plating, magnetic and thermal characterisation, rheological analysis

PACS: 61.46.Fg, 68.37.Lp, 81.07.-b, 81.07.De, 82.35.Np

1 Introduction

The investigation of effective through-service remanufacturing technologies for on-platform repair is of great interest for aerospace applications. Examples of advanced composite repairs for scarf and sandwich panels are shown in Figure 1. However, the conventional methodologies are labour intensive, and therefore costly and time consuming. They are also inefficient in terms of energy delivery in the course repair, suffer from non-uniform temperature distributions, and result in inconsistent levels of curing where part thicknesses are variable, all of which ultimately lead to compromised performance of the repaired components. The present work explores a route towards more controlled curing process. The research focuses on manipulation of nano fillers, such as multi-walled carbon nanotubes (MWCNTs), in host composite structures exposed to external energy fields (specifically electromagnetic fields) for advanced curing purposes. In this regard, the replacement of a damaged composite part, using repair patches, is vital for the restoration of the original performance; this depends crucially on the network generation at the bondline between the original structure and the replacement. The nanotube networks are known to have great potential to improve the through-thickness thermal conductivity (which is essential for uniformity of temperature), and electrical conductivity (which is critical for induction heating) of the composite laminates; these conductivities are low even in the case of carbon fibre composites, since the through-thickness properties are primarily determined by matrix performance. Previous studies [1–3] have demonstrated the importance of the nano filler networks for several applications. Network optimisation would therefore help to accelerate the internal heat supply, decrease temperature gradients along the bondline, evacuate heat upon cooling, and eventually avoid exothermic reactions.

The formation of conductive networks can be realised through manipulation of magnetically sensitive nanofibres (MWCNTs) through external DC magnetic fields. The obtained architecture of percolative nano-reinforcements leads to increases in the local electrical and thermal con-

***Corresponding Author: G. Ariu:** Advanced Composite Centre for Innovation and Science (ACCIS), University of Bristol, BS8 1TR, Bristol, UK, E-mail: giampaolo.ariu@bristol.ac.uk
I. Hamerton, D. Ivanov: Advanced Composite Centre for Innovation and Science (ACCIS), University of Bristol, BS8 1TR, Bristol, UK

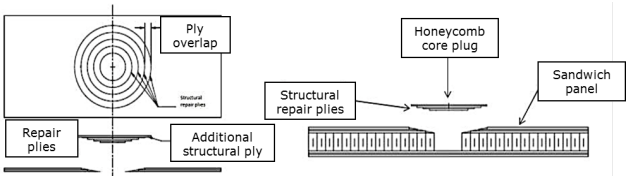

Figure 1: Advanced composite scarf (left) and sandwich panel (right) repair.

ductance. This is particularly important in the areas where there are connections between the host composite plies at the bondline. A schematic is shown in Figure 2.

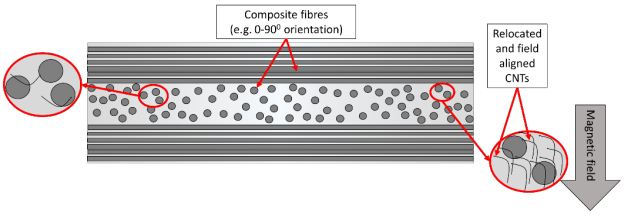

Figure 2: Schematic of composite inner structure for fibre alignment by external energy fields.

Magnetic field manipulation of short fibres has already been investigated in the literature [4–8]. The current project investigates the feasibility of using magnetic fields for both alignments and induction-assisted heating. This is realised through the combination of magnetic field manipulation before resin gelation under a direct current (DC) field, and induction heating via alternating current (AC) fields. The induction-heating phenomenon, widely reported in the literature for different purposes [9–14], can therefore be exploited in order to control the heat generation across specific regions, such as the bondline. This can ensure the most effective repair for structural purposes, with a faster, energy-efficient technique, as reported in the literature for repair of aluminium components [15] and composite joints [16].

2 Experimental

2.1 Equipment

This study used: (a) equipment for functionalizing CNT such as a hot plate magnetic stirrer, sonicator and chemical reagents for the plating steps; (b) equipment for characterization of functionalised particles: Transmission Electron Microscopy (TEM) and Scanning Electron Microscopy (SEM) microscopy; (c) equipment for processing the investigated nanocomposites: shear homogenizer IKA T10 basic ULTRA-TURRAX; (d) physical characterization of the obtained metal functionalised CNT solutions: Differential Scanning Calorimetry (DSC), rheometry, Vibrating Sample Magnetometer (VSM); (e) magnetic set-up for alignment and positioning of the CNT particles; (f) Computerised Tomography (CT) scans for characterisation of the alignment and positioning of the metal-plated CNTs within a viscous medium.

The magnetic apparatus for generating DC fields is shown in Figure 3: there are 9800 turns in the magnetic coils and the total electric current through the coils reaches 1.5 A. The magnetic DC field (flux density of 0.5 T) was applied through two parallel square magnetic poles (pole edge size equal to 25.4 mm). This was used in order to align metal functionalised CNTs within a viscous medium.

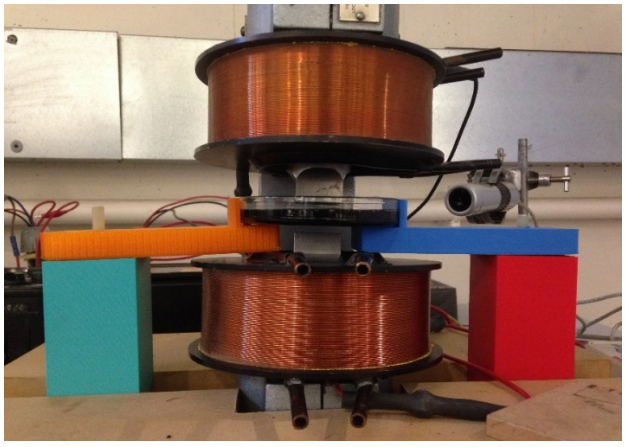

Figure 3: DC magnetic apparatus.

Functionalised CNTs were characterized using Transmission Electron Microscopy (TEM) JEOL JEM-1400. Droplets of examined solutions were prepared from powdered nanotubes and subjected to an ultrasonic bath dispersion in ethanol, prior to the TEM analysis. Rheological measurements were carried out using a cone/plate viscometer (Kinexus, Malvern). Samples containing 2.5 wt.% and 5 wt.% (approximately 5 vol.% and 10 vol.%, respectively) of metal functionalised carbon nanotubes in PRIME^{TM} 20LV (magnetically stirred plating step) were prepared as mixed solutions immediately prior to the tests. These solutions were analysed under application of shear rates ranging from 0.1 s^{-1} to 100 s^{-1} (calculated automatically by the rheometer at the furthest gap location between cone and plate, equal to 0.15 mm). Computerised tomography (CT) scans were carried out using a Nikon XTH225ST

CT Scanner. This technique relies on the application of X-rays for the 2D characterisation throughout the sample and, ultimately, the combination of the 2D scans to obtain the 3D sample mapping. Samples presented circular epoxy resin/MWCNT tabs with diameter of 35 mm and thickness of 10 mm. These tests were carried out in order to assess the CNT alignment within the epoxy resin following the externally applied magnetic field and the related edge effects. Magnetic characterisation was performed using a vibrating sample magnetometer (VSM), wherein samples (solid or fluid), located between parallel pickup coils, were mechanically excited at a known frequency and simultaneously subjected to a uniform DC field, ranging from −0.1 T to 0.1 T. The detection of the magnetic field level occurs using a Gauss meter placed on the magnetic poles of the apparatus [17]. Thermal characterisation was carried out on samples (10-15 mg) in hermetically sealed pans using modulated differential scanning calorimetry (MDSC, TA Instruments Q200). Samples were equilibrated at the initial temperature of 20°C with a modulation of ±1.00°C for 60 seconds, followed by a ramp rate of 5 K/min to reach the final temperature of 180°C.

2.2 Materials

Several carbon nanotube configuration were used in this study:

1. Multi-wall carbon nanotubes (MWCNTs) (manufactured by Sigma Aldrich) were characterised by high aspect ratios (around 1500; cross-section diameter of 6-13 nm). Electroless plating of these carbon nanotubes is described in the next paragraph.
2. Commercial nickel-coated nanotubes (manufactured by US Research Nanomaterials, Inc.) were purchased. These CNTs exhibit purity higher than 98%, outer diameters of 5-15 nm and aspect ratios higher than 1000.

The low-viscosity host epoxy resin system was PRIME^{TM} 20LV (manufactured by Gurit) designed for liquid moulding processes. The epoxy comprises a slow amine hardener, has a viscosity of 1010-1070 cP at 20°C, and a cure schedule of 7 hours at 65°C as per supplier's instructions.

2.3 Electroless plating of multi-walled carbon nanotubes

An electroless plating technique was used to deposit homogeneous, chemically-stable, metal functionalised coatings (e.g. nickel, cobalt, and nickel-iron) on the sides and ends of the MWCNTs [18, 19]. The procedure for Ni/Co deposition involved a nanotube sensitization step with tin(II) chloride, an activation step involving palladium(II) chloride, and a plating bath under sonication or magnetic stirring forces. The latter required the use of a reducing agent (hypophosphite), a complexing agent (citrate) and the metal salt to be reduced on to the nanotubes under specific pH and temperature conditions [20]. Nanotube aspect ratio was significantly reduced during the sensitization and activation steps which involved a sonication process. This phenomenon could therefore facilitate the final plating step for the nanotube metal functionalization, whilst reducing nanotube bending and fracture during incorporation within a host medium via sonication. A schematic of the electroless plating process is shown in Figure 4.

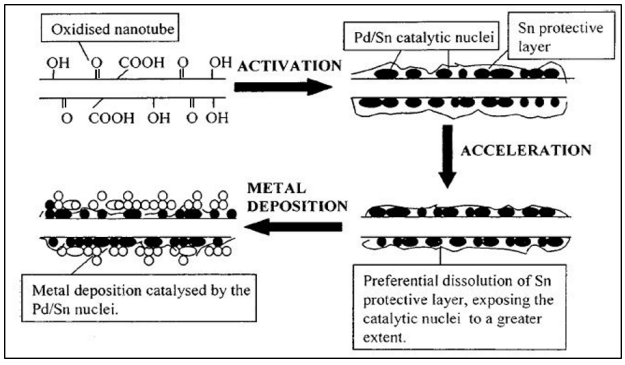

Figure 4: Schematic of electroless plating technique [19].

2.4 Blending of MWCNTs and alignment

The metal-functionalised MWCNTs were introduced into the epoxy at a volume fraction of 2.5 wt.% within a circular mould (outer diameter of 92 mm; thickness of 10 mm), and shear mixing (5000 rpm for 1 hour) was used to effect dispersion. The slow amine hardener was added to the suspension in order to facilitate the chemical crosslinking of the polymeric chains. The blends were then exposed to a magnetic DC field with flux density of 0.5 T, until gel time was reached after around 200 minutes.

3 Results and discussion

3.1 Deposition of metal particles on MWCNTs

Several metal plating methodologies were investigated, including nickel, cobalt and nickel-iron plating. The aim of metal functionalisation was to increase the magnetic sensitivity of the nanotubes. The functionalized MWCNTs were characterized using TEM to investigate the position and density of metal particles. Commercial nickel-coated nanotubes were compared to nickel-plated nanotubes prepared experimentally in-house, to visually assess the integrity and the distribution of the nickel-coating along the length of the nanotubes. Nanotube micrographs for the commercial nickel-coated and nickel-plated nanotubes are shown in Figure 5; dark regions and spots in the micrographs represent the metal nanoparticles on the walls of the nanotubes. It is evident from Figure 5(a), that the heterogeneous nickel coating distribution reflects the poor adhesion of the coating, regardless of the coating process. In contrast, Figure 5(b) shows more uniform wall coating distribution for single MWCNTs. Figure 5(c) shows the micrograph related to cobalt-plated MWCNTs. The latter were obtained through a magnetically stirred plating bath. Agglomeration greatly influences the nanotube distribution. However, both nickel and cobalt seem to provide the nanotubes with satisfactory coating adhesion and uniform distribution, although to a lower extent for the cobalt-plated nanotubes; this is potentially due to the magnetic stirring process. Nanotube agglomeration represents a well-known phenomenon, which is not necessarily detrimental to the overall component electrical performance [21].

3.2 Rheological characterization of epoxy-MWCNT blends

Rheological measurements were carried out in order to investigate the flow properties of the metal-plated CNT-filled resin systems. Plots of shear viscosity (in Pa·s) as a function of the shear rate (in s^{-1}) are shown in Figure 6 for Co30- and carboxyl-functionalised nanotubes embedded in PRIME^{TM} 20LV. Results are reported on a log-log plot. The introduction of MWCNTs in the epoxy resin causes a pronounced increase in viscosity, leading to a viscosity difference of about 200% between the neat resin and the solutions containing metal-plated CNTs, as expected. The variation in viscosity in the range of 2.5-5% weight fraction of

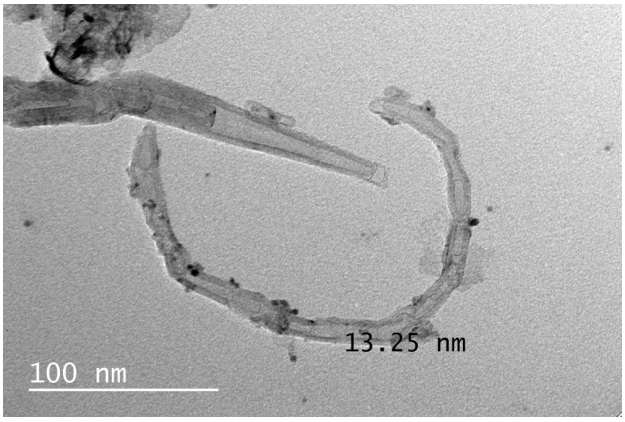

(a)

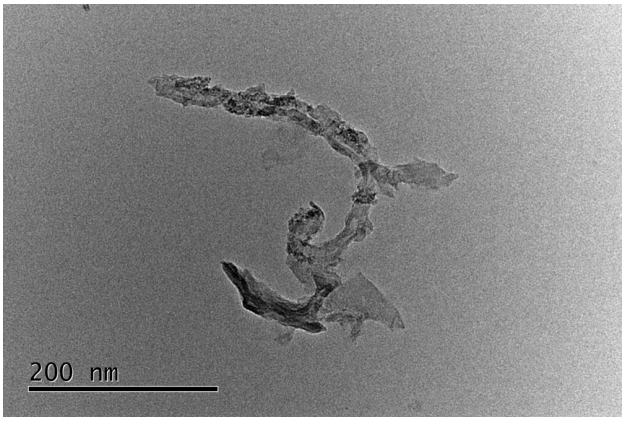

(b)

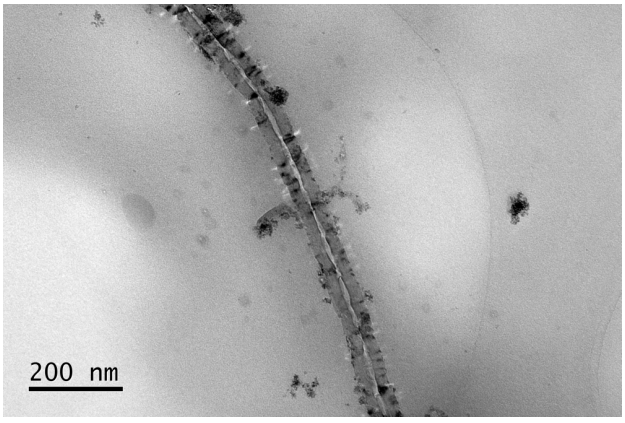

(c)

Figure 5: TEM comparison between commercial Ni-coated (a), Ni-plated (b), and Co-plated (c) MWNTs (please note different scales on the micrographs). Ni-coated (a) nanotube diameter value was obtained qualitatively via ImageJ software.

CNTs and different types of CNTs appears much smaller than the drop in viscosity due to shear thinning at the rates of 0.1-50 1/s. Therefore, the shear rate plays a significant role in the shear viscosity changes; increasing shear rates

could ease the processability of the nanotube-filled resin systems due to shear-thinning effects.

The manipulation of the metal-plated nanotubes within epoxy resin under magnetic field was then investigated for the generation of well-ordered networks for the increase in local conductivity.

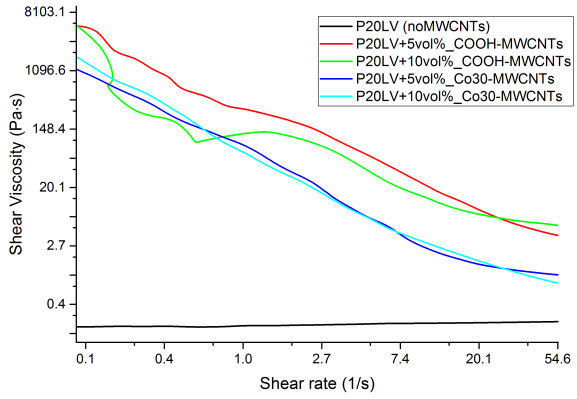

Figure 6: Shear viscosity as a function of shear rate for 5 vol.% and 10 vol.% of COOH-MWCNTs and Co30-MWCNTs in PRIME^{TM} 20LV.

3.3 Cure kinetics characterization of the epoxy-MWCNT blends

Preliminary MDSC analyses [22] were performed on nanocomposite systems with low-viscosity epoxy resin PRIME^{TM} 20LV (plus amine hardener) containing 2.5 wt.% (approximately 5 vol.%) of metal functionalised MWCNTs. The total and reversing heat flow obtained could help to assess the influence of the presence of nanotubes, and added metal functionality, on the thermal behaviour of the system. Figure 7 shows the preliminary total heat flow results from the analysis performed at a ramp rate of 5 K/min.

Neat resin results were considered as a baseline for the assessment of thermal changes due to the presence of the carbon nanotubes. An endothermic peak at 23°C could be observed: this was related to the nanotube dispersion (bond breakage and macroscopic reorganisation) within the resin system, which requires an additional external heat supply. However, the onset of the exothermic peak, due the resin cure process, clearly showed a shift towards lower temperatures for the metal-functionalised nanotubes. Moreover, the peak intensity increased for the metal-plated nanotubes. Therefore, the beneficial effect of the nanotubes to the cross-linking process can be stated, in particular for Ni-plated nanotubes. In this case, the ap-

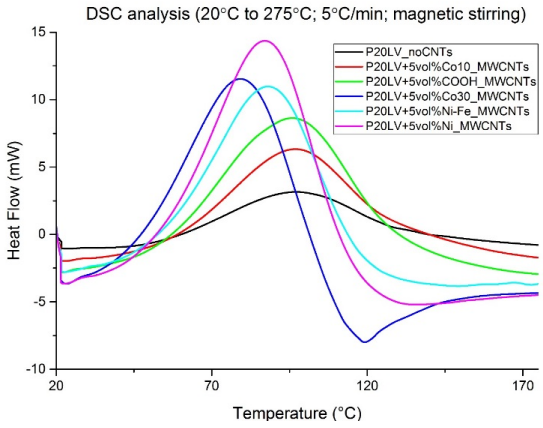

Figure 7: Comparison of PRIME^{TM} 20LV/amine/MWCNT (2.5 wt.%, approximately 5 vol.%) blend reactivity using MDSC (5 K/min.).

propriate balance of carboxyl functional groups and nickel nanoparticles leads to the highest compatibility and stability with the host matrix, which is represented by the higher exothermic heat value.

The introduction of metal-functionalised carbon nanotubes clearly has an effect on the gelation and cross-linking process occurring in the resin. The exothermic energies related to the MDSC curves are shown in Figure 8. These figures were obtained by taking into consideration both the epoxy equivalent weight, and the amine equivalent weight, in the samples tested with MDSC. The introduction of MWCNTs in PRIME^{TM} 20LV causes an increase in the exothermic heat generated during polymerisation compared to the neat resin. However, the carboxyl-functionalised nanotubes show the highest energy levels (around 55 kJ/mol), although the onset of the exothermic peak appears at higher temperatures, compared to the case of metal-plated nanotubes (except the Co10-plated CNTs; the '10' represents the nanotubes were collected after 10 minutes of cobalt plating). This could be related to the fact that metal nanoparticles on nanotubes accelerate the creation of reactive regions with the polymeric chains, but their chemical compatibility with the epoxy resin is lower than the compatibility between carboxyl groups and epoxy. Nonetheless, the introduction of metal-plated MWCNTs could be exploited for manipulating and optimising the curing process during repairs.

3.4 Determining the magnetic susceptibility of the blends

Metal-plated, carboxyl-functionalised MWCNTs as dry powder were characterised using VSM. Several key mag-

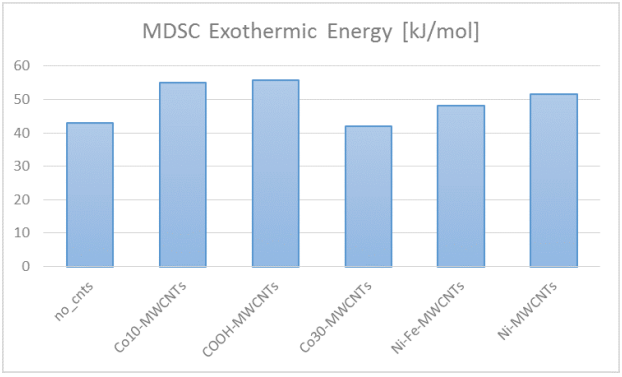

Figure 8: Comparison of heats of polymerisation for the different epoxy blends.

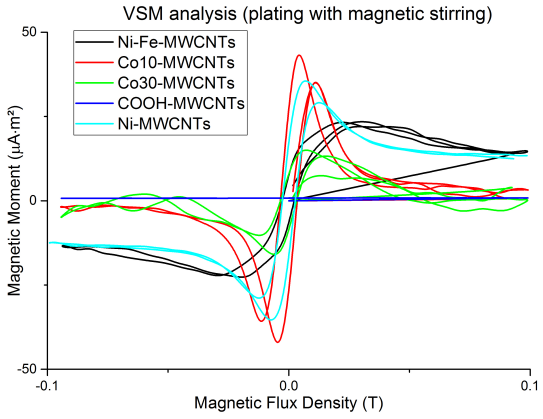

(a)

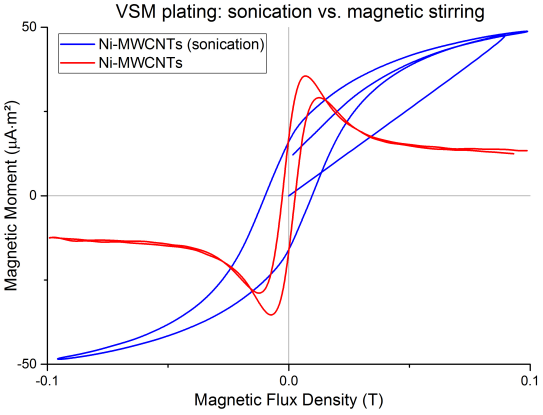

(b)

Figure 9: (a) VSM results and (b) plating/stirring comparison for Ni-plated MWCNTs.

netic properties, such as magnetisation and magnetic moment, were determined as a function of the externally applied magnetic field (the applied DC field ranging from −0.1 T to 0.1 T). The graph in Figure 9(a) shows the results from the magnetic analysis. Specifically, Co10 and Co30 represent the cobalt-plated nanotubes obtained after 10 and 30 minutes of plating, respectively. The Co10- and nickel-plated nanotubes showed the highest magnetic moments at low magnetic flux densities, but the magnetic moment decreased significantly at higher flux densities in both cases. Indeed, the heterogeneity of the coating on the nanotube walls, and among several nanotubes and their agglomerates, reflects the presence of poorly functionalised nanotube regions, which can be magnetically sensitive at higher field levels. The decrease in magnetic moment, particularly for Co10, indicates that the magnetically-stirred plating bath provides lower magnetic properties than other procedures, such as the sonicated bath. As expected, the nanotubes tend to cluster in proximity to the magnetic stirrer, therefore providing a film resistance counteracting the functionalisation of the surrounding nanotubes. As a result, magnetic gradients between single nanotubes or agglomerates become relevant in the investigated samples.

Figure 9(b) shows the magnetic properties for nickel-functionalised carbon nanotubes after exposure to a sonicated and magnetically stirred plating bath. The dependence of the magnetic moment on the applied flux density, for the sonicated nickel-plated nanotubes (blue line in Figure 9(b)), shows three distinct regions: magnetisation at increasing flux densities, magnetic saturation for flux densities approaching 0.1 T, and magnetic remanence when the field is no longer applied. The magnetic remanence is not influenced by the plating procedure, although the magnetic moment and saturation clearly benefit from the plating bath homogenisation imposed through sonication. Magnetic moment values for Ni-plated nanotubes after sonication approach 50 $\mu A \cdot m^2$, whereas after a magnetically stirred plating bath, the magnetic moment does not exceed 30 $\mu A \cdot m^2$. Different scenarios can be observed for Co-plated and Ni-Fe-plated MWCNTs (Figure 10): in the first case, the plating procedure alters the magnetic remanence and the coercivity.

Moreover, Co-plated nanotubes obtained using a sonicated bath show a higher magnetic moment, around 160 $\mu A \cdot m^2$, which represents the highest figure achieved among the investigated nanotube coatings. Additionally, the extremely low coercivity of sonicated Co-plated nanotubes favours the magnetisation changes and, therefore, the hysteresis loss generation, although the hysteresis loop shown in Figure 10 is relatively small. On the other hand, the influence of the plating methodology on the magnetic properties of the nanotubes is negligible in the case of Ni-Fe-plated MWCNTs. Further investigation is required for the electroless plating of carbon nanotubes with

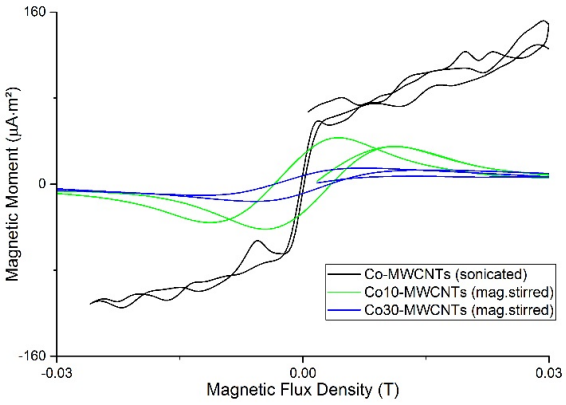

Figure 10: Vibrating Sample Magnetometer plating/stirring comparison for Co-plated MWCNTs.

metal compounds. The influence of the metal-plated nanotubes on the flow properties of the matrix will be investigated in the next section as a means to assessing the processability of the system.

3.5 Magnetic alignment of the coated and uncoated MWCNTs

Initial work consisted of modelling analysis and experimental validation for the magnetic field manipulation of non-functionalised MWCNTs in low-viscosity epoxy resin, for alignment and network-generation purposes. Magnetic equipment (Figure 3), was used for the through-thickness nanotube alignment in the epoxy resin. Approximated values of magnetic flux density for the alignment of uncoated nanotubes in PRIME^{TM} 20LV were in the range of 0.5-0.7 T. This finding provided a guideline for the design of a magnetic DC setup used for further experimental analysis. The epoxy/MWCNT blends were exposed to a magnetic DC field, with flux density of 0.5 T until gel time was reached after around 200 minutes.

Nickel-plated and carboxyl-functionalised MWCNTs, obtained through a sonicated plating bath, were introduced in low-viscosity epoxy resin (PRIME^{TM} 20LV with amine hardener) with a weight fraction equal to 2.5 wt.%. The sample holder had an outer diameter of 35 mm and thickness of 10 mm. Both nanotube types were subjected to an external magnetic field, with a flux density of 0.5 T in the first instance. Consequently, further analysis involved the application of lower fields of 0.25 T and 0.1 T to two samples, with 2.5 wt.% of nickel-plated nanotubes in PRIME^{TM} 20LV, in order to investigate the nanotube magnetic alignment at different field levels. The field was held until gelation occurred. Samples were then allowed to cool naturally to room temperature, in order to complete the resin cure. No external heat sources were applied during the field application, although the magnetic setup may have heated up, due to internal coil resistance, and accelerated the gelation process. Computerised tomography (CT) scans were carried out for those nickel-plated reinforced epoxy systems subjected to flux densities of 0.25 T and 0.5 T. Qualitative assessments of the preferential distribution and through-thickness alignment of the nickel-plated and carboxyl-functionalised MWCNTs were conducted. Figure 11(a) shows the epoxy/nickel-plated nanotube samples subjected to different magnetic field levels; the square alignment pattern can be observed. However, a more detailed CT analysis through is required.

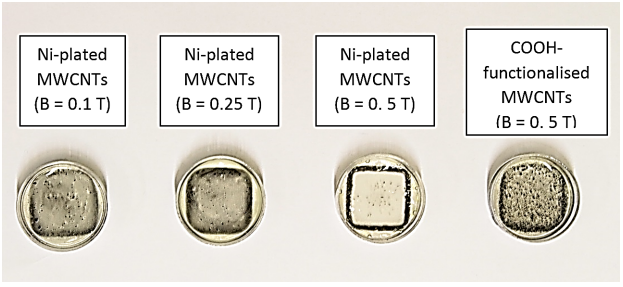

(a)

(b)

Figure 11: (a) Ni-plated MWCNTs alignment comparison after DC field and (b) CT scan of PRIME^{TM} 20LV+2.5 wt.% Ni-plated MWCNTs under 0.5 T.

Figure 11(b) shows the CT scan for nanocomposite systems characterised by the presence of 2.5 wt.% of Ni-plated MWCNTs in PRIME^{TM} 20LV. The scans were obtained on the cured samples. The samples were first subjected to different DC fields, 0.25 T and 0.5 T, using the manufacturer's recommended gel time. Subsequently, curing was carried

out at room temperature, and the nanotubes and nanotube agglomerates can be observed distributed in a square pattern. The pattern reflects the magnetic pole geometry, and the presence of edge effects. The magnetic field reaches its highest value at the edge of the magnetic poles, where the magnetic domains are not counterbalanced by adjacent neighbours, as in the magnetic bulk. Finite element analysis was carried out using Finite Element Methods Magnetics (FEMM) to replicate the magnetic field application through the thickness of the samples as shown in Figure 12.

The air gap between the poles, *g*, was equal to 28 mm, whereas the magnetic pole in-plane size, *p*, was 25.4 mm. The magnetic flux density mapping (Fig. 12) shows a gradient between the centre and the edges of the poles, from yellow to purple respectively. Specifically, the increase in magnetic flux density at the pole edges is around 40% compared to the pole centre, which leads to an inhomogeneous magnetic field responsible for the alignment pattern. A more enhanced alignment pattern can be obtained through the application of a stronger field, as expected and shown in Figure 11. This phenomenon proves the potential manipulation of metal-functionalised nanotubes in low-viscosity mediums (i.e. PRIME^{TM} 20LV with addition of amine hardener) *via* external magnetic fields. Further investigation is required into nanotube manipulation in higher viscosity systems, e.g. with the presence of structural fibres in fibre-reinforced polymer composites.

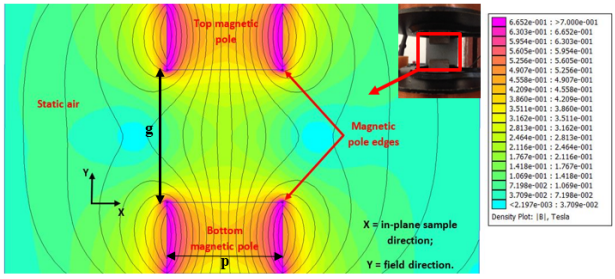

Figure 12: Finite Element Methods Magnetics (FEMM) model showing the magnetic flux density gradient between the edges and centre of the DC magnetic poles.

4 Conclusions

The study has shown that an external magnetic field has great potential for positioning and alignment of CNTs. The study has demonstrated the feasibility of creating well-ordered architectures with an unprecedented level of control of network geometry. Various methods of functionalisation and various metal additives were considered. The microstructural and VSM analysis revealed that the most promising system was cobalt-functionalised nanotubes obtained using the electroless plating technique. This methodology allows for a more uniform coating on the nanotube walls than is currently obtained in commercially available metal-coated nanotubes. Magnetic characterisation indicated that cobalt-plated nanotubes showed the highest magnetic moment (around 160 $\mu A \cdot m^2$) and lowest coercivity, making these the most suitable for alignment, positioning and induction heating. Although introduced at volume fractions up to 5 wt.% (approximately 10 vol.%), the metal-plated nanotubes did not hinder the resin processability, especially at relatively high shear rates, as shown from rheological measurements. There is a room for further optimization of metal coatings, and their influences on nanocomposite thermal and rheological properties. The potential use of these nanocomposite systems for induction heating purposes was validated by thermal analysis. In particular, carboxyl-functionalised nanotubes showed the highest energy levels (around 55 kJ/mol), which could be associated with the fact that metal nanoparticles on nanotubes accelerate the creation of reactive regions with the polymeric chains. However, their chemical compatibility with the epoxy resin was lower than the compatibility between carboxyl groups and epoxy. Nonetheless, this will be of great importance for an optimised control of the curing process, supported by the use of dielectric resins. This is study offers a first step towards proof of concept as a novel repair technology. This will need to be applied to more industrially relevant resins, which are generally of higher viscosity; the influence of the metal-plated MWCNTs on the thermal properties of the resin will be investigated further as a cure-control tool for high performance of the final part, especially at the bondline. Alternative methods, such as fuzzy fibres [23], could be used to increase the through -thickness electrical conductivity, which can help create high-conductivity paths.

Acknowledgement: The authors would like to acknowledge support from Rolls-Royce plc, particularly Mr. Paul Williams and Ms. Bhrami Jegatheeswaram Pillai, for this research through the Composites University Technology Centre (UTC) at the University of Bristol, and from the Engineering and Physical Sciences Research Council (EPSRC) through the Centre for Doctoral Training in Advanced Composites at the University of Bristol (Grant no. EP/L016028/1). The authors would also like to acknowledge Dr. Jacopo Ciambella from the "Sapienza" University of Rome for the greatly appreciated technical support at the start of the project.

References

[1] Yan, X. *et al.* (2016) Lowly loaded carbon nanotubes induced high electrical conductivity and giant magnetoresistance in ethylene/1-octene copolymers. Polymer. 103: 315-327.

[2] Wu, K. *et al.* (2016) Largely enhanced thermal and electrical conductivity via constructing double percolated filler network in polypropylene/expanded graphite - Multi-wall carbon nanotubes ternary composites. Composites Science and Technology. 130: 28-35.

[3] Lian, G. *et al.* (2016) Vertically Aligned and Interconnected Graphene Networks for High Thermal Conductivity of Epoxy Composites with Ultralow Loading. Chemistry of Materials. 28: 6096-6104.

[4] Kimura, T. *et al.* (2002) Polymer Composites of Carbon Nanotubes Aligned by a Magnetic Field. Advanced Materials. 14 (19): 1380-1383.

[5] Erb, R. M. *et al.* (2012) Composites reinforced in three dimensions by using low magnetic fields. Science. 335(13): 199-204.

[6] Choi, E. S. *et al.* (2003) Enhancement of thermal and electrical properties of carbon nanotube polymer composites by magnetic field processing. Journal of Applied Physics. 94(9): 6034-6039.

[7] Goc, K. et al. (2016) Influence of magnetic field-aided filler orientation on structure and transport properties of ferrite filled composites. Journal of Magnetism and Magnetic Materials. 419: 345–353.

[8] Le Ferrand, H. *et al.* (2016) Magnetic assembly of transparent and conducting graphene-based functional composites. Nature Communications. 7: 1-9.

[9] Mas, B. *et al.* (2013) Thermoset curing through Joule heating of nanocarbons for composite manufacture, repair and soldering. Carbon. 63: 523–529.

[10] Bayerl, T. *et al.* (2014) The heating of polymer composites by electromagnetic induction - A review. Composites Part A: Applied Science and Manufacturing. 57: 27–40.

[11] El-Tantawy, F. *et al.* (2003) A novel way of enhancing the electrical and thermal stability of conductive epoxy resin–carbon black composites via the Joule heating effect for heating-element applications. Journal of Applied Polymer Science. 87: 97-109.

[12] Fink, B. K. *et al.* (1992) A Local Theory of Heating in Cross-Ply Carbon Fiber Thermoplastic Composites by Magnetic Induction. Polymer Engineering & Science. 32: 357–369.

[13] Yarlagadda, S. *et al.* (2002) A study on the induction heating of conductive fiber reinforced composites. Advanced Composite Materials. 11(1): 71-80.

[14] Abliz, D. *et al.* (2013) Curing Methods for Advanced Polymer Composites - A Review. Polymers & Polymer Composites. 21(6): 341-348.

[15] Kim, M. *et al.* (2014) Repair of aircraft structures using composite patches bonded through induction heating. Advanced Composite Materials. 24(4): 307-323.

[16] Mahdi, S. et al. (2003) A Comparison of Oven-cured and Induction-cured Adhesively Bonded Composite Joints. Journal of Composite Materials. 37(6): 519-541.

[17] Foner, S. (1996) The vibrating sample magnetometer: Experiences of a volunteer (invited). Journal of Applied Physics. 79(8): 4740-4745.

[18] Grzelczak, M. *et al.* (2007) Pt-Catalyzed Formation of Ni Nanoshells on Carbon Nanotubes. Angewandte Chemie International Edition. 46: 7156-7160.

[19] Sun, Y.-P. *et al.* (2002) Functionalized Carbon Nanotubes: Properties and Applications. Accounts of Chemical Research. 35: 1096-1104.

[20] Li, Q. *et al.* (1997) Coating of Carbon Nanotube with Nickel by Electroless Plating Method. Japanese Journal of Applied Physics. 36 (2): 501-503.

[21] Seidel, G. D. *et al.* (2008) Analysis of Clustering and Interphase Region Effects on the Electrical Conductivity of Carbon Nanotube-Polymer Nanocomposites via Computational Micromechanics. ASME Proceedings |Multifunctional Materials: 159-165.

[22] Ozawa, T. (2000) Thermal analysis — review and prospect. Thermochimica Acta. 355(1-2): 35-42.

[23] Pozegic, T. R. *et al.* (2014) Low temperature growth of carbon nanotubes on carbon fibre to create a highly networked fuzzy fibre reinforced composite with superior electrical conductivity. Carbon. 74: 319-328.